Materials Science-Poland, *Vol. 26*, *No. 4*, *2008*

Magnetism of ultra-thin iron films seen by the nuclear resonant scattering of synchrotron radiation

T. ŚLĘZAK[1*], S. STANKOV[3], M. ZAJĄC[1], M. ŚLĘZAK[1], K. MATLAK[1], N. SPIRIDIS[2], B. LAENENS[4], N. PLANCKAERT[4], M. RENNHOFER[5], K. FREINDL[2], D. WILGOCKA-ŚLĘZAK[2], R. RÜFFER[3], J. KORECKI[1, 2]

[1]Faculty of Physics and Applied Computer Science, AGH University of Science and Technology, al. Mickiewicza 30, 30-059 Cracow, Poland

[2]Institute of Catalysis and Surface Chemistry, Polish Academy of Sciences, ul. Niezapominajek 8, 30-239 Cracow, Poland

[3]European Synchrotron Radiation Facility, BP220, F-38043 Grenoble, France

[4]Instituut voor Kern- en Stralingsfysica, K.U.Leuven, Celestijnenlaan 200D, B-3001 Leuven, Belgium

[5]Fakultät für Physik, Universität Wien, Strudlhofgasse 4, A-1090 Wien, Austria

Conversion electron Mössbauer spectroscopy proved in the past to be very useful in studying surface and ultrathin film magnetism with monolayer resolution. Twenty years later, its time-domain analogue, the nuclear resonant scattering (NRS) of synchrotron radiation, showed up to be by orders of magnitude faster and more efficient. The most important features of NRS based on simulations and experimental data have been discussed. It has been shown how the isotopic sensitivity of NRS, combined with the ^{57}Fe probe layer concept, was explored to study influence of the interlayer exchange coupling to FeAu monoatomic superlattices on the magnetic properties of the iron monolayer on Au(001). In the second example, combination of UHV conditions and the high brilliance of the third generation synchrotron source is used to probe the evolution of spin structure in epitaxial Fe films on W(110) via the accumulation of high quality time spectra directly during the ^{57}Fe film growth.

Key words: *thin films; magnetism; nuclear resonant scattering; synchrotron radiation; Fe(001)/Au(001); Fe(110)/W(110)*

1. Introduction

Magnetic properties of nanoscale materials are nowadays of great scientific and technological interest. Complex magnetic structures often found in low-dimensional

*Corresponding author, e-mail: slezak@uci.agh.edu.pl

systems, such as ultra-thin iron films, present a challenge for experimental methods. They have been studied by scanning probe microscopy (SPM) [1], spin sensitive electron scattering techniques [2], X-ray magnetic dichroism [3], magneto-optic Kerr effect (MOKE) [4], magnetometry [5], and ^{57}Fe conversion electron Mössbauer spectroscopy (CEMS) [6]. Except the last one, all these methods suffer from limited depth resolution: spin-polarized scanning tunneling is strictly surface sensitive, while the others integrate magnetic properties over the entire sample or over an element. From this point of view, CEMS and, recently, the grazing incidence nuclear resonant scattering (NRS) of synchrotron radiation are exceptional since, owing to their isotopic selectivity, they make it possible to study magnetic properties with spatial resolution using isotopic probe-layers.

NRS is a synchrotron analogue the of Mössbauer spectroscopy (MS), in the sense that recoilless excitation (induced by the resonant X-rays with energy 14.4 keV for ^{57}Fe) of the nuclear energy levels, split due to the hyperfine interactions, is involved. In this method, the hyperfine parameters can be obtained from a characteristic beat pattern seen in the time evolution of the intensity of nuclear resonant scattering (the so called time spectrum). In conventional MS methods, such as conversion electron Mössbauer spectroscopy (CEMS), the hyperfine interactions are measured in an incoherent process, in which the decay of a nucleus resonantly excited by a γ-quant occurs via resonance fluorescence or internal conversion. The resulting spectrum is the incoherent sum of those single events. In contrast, the NRS signal, measured after a simultaneous excitation of an ensemble of nuclei by a synchrotron radiation pulse, results from the coherent superposition of the probability amplitude for scattering from all nuclei of the ensemble. This coherent character of the scattering process, in combination with the outstanding properties of the synchrotron radiation from third generation synchrotron sources (high brilliance, tunability in energy with monochromatization down to 0.5 meV, defined time structure, and polarization) opened new possibilities for time resolved nuclear spectroscopy based on hyperfine interactions. Magnetic properties in the nanoscale can be studied with sub-monolayer sensitivity. The isotopic sensitivity, in combination with the ^{57}Fe probe layer concept, gives local structural and magnetic information from a sample region pre-selected during the preparation process. Furthermore, the well defined polarization of the synchrotron X-rays allows for an enhanced (with respect to CEMS) sensitivity to the orientation of the hyperfine magnetic field and electric field gradient. Extensive description of the method and its application can be found in several review papers [7] and a comprehensive book [8]. The aim of this paper is to present capabilities of the method in studying ultrathin Fe film, especially *in situ*, under ultrahigh vacuum (UHV) conditions, which became possible thanks to recent experimental developments at the beamline ID18 at European Synchrotron Radiation Facility (ESRF) in Grenoble.

2. Experimental method

NRS on thin films or surfaces is a nuclear diffraction technique performed under specular reflection geometry at grazing incidence (GI) as shown in Fig. 1. A newly constructed UHV system [9] at the beamline ID 18 at ESRF Grenoble [10] permits GI-NRS experiments *in situ,* and also during or shortly after ^{57}Fe deposition. This multichamber UHV system ensures state-of-the-art preparation and characterization of single crystalline surfaces and epitaxial films, offering evaporation of several metals (including Fe isotopes). There is a portable UHV chamber which enables a sample to be transferred to the system from a remote laboratory (e.g., in Cracow) without exposure to ambient atmosphere. Other sample environments, including a broad range of temperatures and high magnetic fields are available at ID 18 for *ex situ* ultrathin film studies. With the fine focusing of the synchrotron beam down to 30 μm, measurements on wedge samples are possible, and the acquisition time, below one hour for a monolayer of ^{57}Fe and of single minutes for several atomic ^{57}Fe layers, places the method among the most efficient tools for thin film and nanostructure magnetism studies.

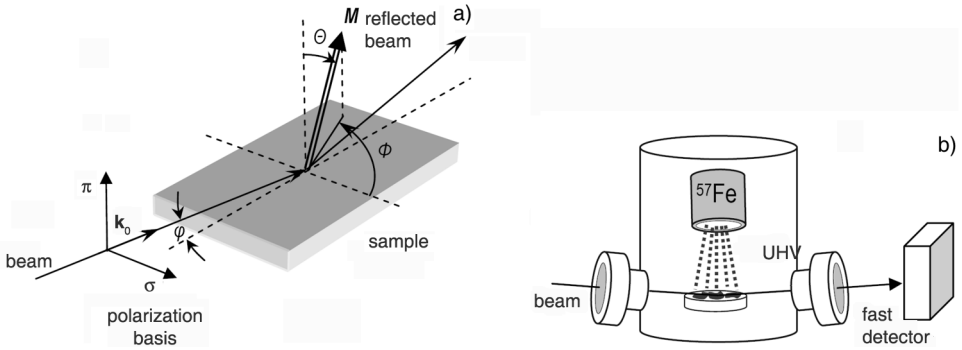

Fig. 1. Geometry of a grazing incidence nuclear resonance scattering experiment (a); angles Θ and Φ give relative orientation of the incident synchrotron beam wave vector $\mathbf{k}_0$ to magnetization M. σ and π are the linear polarization basis vectors. The grazing angle φ is typically a few milliradians (after [12]); scheme of the UHV NRS scattering chamber at ID 18 of the ESRF (b)

The basic features and capabilities of the GI-NRS method can be best visualized via the simulated time spectra for ^{57}Fe films (deposited on a tungsten substrate), shown in Fig. 2. The simulations were done with the program package CONUSS [11] based on the dynamical theory of the nuclear resonant scattering. The grazing angle was fixed to 3.8 mrad, which corresponds to the critical angle of Fe. In Figure 2a, the time spectrum for a ^{57}Fe layer with the thickness L = 15 Å, represented by a single non-magnetic site is shown, revealing an exponential decay of the nuclear excited state with the lifetime of 97 ns. The time spectra in Fig. 2b are for the same layer, but now ferromagnetic, magnetized in plane along the wave vector $\mathbf{k}_0$ of the synchrotron beam that is linearly σ polarized. The spectra plotted with the solid and dashed lines correspond to discrete hyperfine magnetic field B_{HF} = 32 T and to the same field with

a hyperfine field distribution (HFD) of about 5 T, respectively. Both spectra clearly show quantum beats of magnetic origin, but in the case of HFD, the scattered intensity decays considerably faster (so called accelerated decay), and additional low frequency modulation can be seen. From the beat frequency, which is inversely proportional to the magnetic hyperfine field, the B_{HF} value can be precisely determined. The sensitivity of GI-NRS to the orientation of the B_{HF} with respect to the wave vector $\mathbf{k}_0$ of the incoming radiation is clear from the comparison of the time spectra shown in Figs. 2b–d.

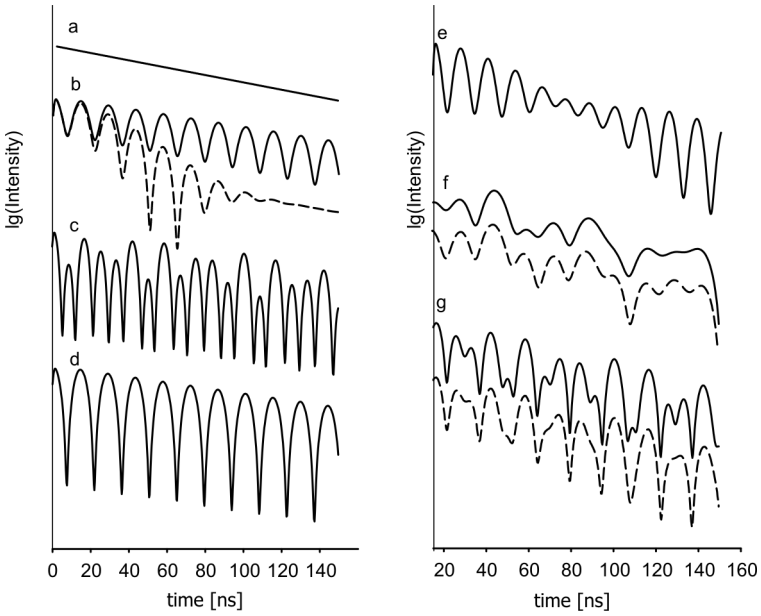

Fig. 2. Simulated GI-NRS time spectra for 15 Å ^{57}Fe layers (L) on tungsten (W): a) non-magnetic case, b) single ferromagnetic layer with the $M \parallel \mathbf{k}_0$ and discrete B_{HF} = 32 T (solid line) or HFD of 5T (dashed line), c) single layer with in-plane B_{HF} = 32 T, perpendicular to $\mathbf{k}_0$, d) single layer with out-of-plane B_{HF} = 32 T, perpendicular to $\mathbf{k}_0$, e) single layer with B_{HF} = 32 T parallel to $\mathbf{k}_0$ and EFG (QS = 0.6mm/s) along the sample normal, f) double layers W/L_1/L_2/ (solid line) and W/L_2/L_1 (dashed line) with B_{HF1} = 32 T and B_{HF2} = 20 T, both parallel to $\mathbf{k}_0$, g) double layers with mutually perpendicular in-plane fields ($B_{HF1} = B_{HF2}$ = 32 T). Solid and dashed lines correspond to different B_{HF} orientation sequences (see text for details)

The beat pattern structure visibly changes for various in-plane orientations of B_{HF}, parallel and perpendicular to $\mathbf{k}_0$ (Fig. 2b, c, respectively), as well as for the out of plane B_{HF} direction (Fig. 2d). Also, the electric field gradient (EFG) alters the time spectrum depending on its value and orientation of main axis as shown in Fig 2e. Modification of the hyperfine pattern by a quadrupole splitting QS = 0.6 mm/s with the main axis of EFG oriented along the sample normal results in an additional beat period superimposed on the high frequency beating of magnetic origin. When the Fe layer becomes thicker, the quantum beat pattern is modified by the so-called dynamical beats related to the collective excitation of the Fe ensemble. Finally, a film composed of two 15 Å thick L_1 and L_2 layers with the hyperfine fields B_{HF1} = 32 T and

B_{HF2} = 20 T parallel to the $\mathbf{k}_0$ is considered. Interestingly, the layer sequence with respect to the substrate clearly influences the shape of the time spectrum, as can be seen from Fig. 2f. The solid line was simulated for the configuration W/L_1/L_2, whereas the dashed line corresponds to the W/L_2/L_1 case. The shape of the time spectrum is also sensitive to the layer sequence when the layers differ only in the direction of their hyperfine fields. This is demonstrated in Fig. 2g where the time spectrum for a system W/L_1/L_2 (B_{HF1} = B_{HF2} = 32 T) with the layer closer to the substrate magnetized parallel to $\mathbf{k}_0$, and the other, magnetized also in the film plane but perpendicular to $\mathbf{k}_0$ (solid line), is compared with that for the opposite situation (dashed line). Such a depth sensitivity of GI-NRS results from the small penetration depth of X-rays at the grazing incidence and enhanced contribution of the Fe atoms located closer to the sample surface with respect to the buried ones. While this effect is negligible for films in Ångstrom thickness range, it becomes essential for thicknesses of even a few nanometers.

It has to be remembered that the complexity of the GI-NRS spectra for real samples goes much beyond the simple pictures discussed above. Since the scattering amplitudes add coherently, the interference from different sites leads to complicated time spectra, especially when energy and angular distributions of the hyperfine parameters are involved. Although it was shown by Röhlsberger et al. [12] that, for ultra thin ^{57}Fe films (below 2 nm), a kinematic approach can be used, the extraction of the full magnetization structure for complex systems is not obvious and unambiguous. In such cases, information from the classical Mössbauer spectrum, if available, is very helpful.

In order to demonstrate unique features of the GI-NRS technique, we will focus on the experimental data obtained for epitaxial Fe/Au and Fe/W nanostructures.

3. Fe/Au nanostructures

In the *ex situ* Fe/Au experiment, the isotopic sensitivity of GI-NRS, combined with the ^{57}Fe probe layer concept, were explored to study changes in the magnetic properties of a single Fe monolayer on Au(001) induced by the interlayer exchange coupling (IEC) to FeAu monoatomic superlattices [13]. The studied system, prepared using UHV molecular beam epitaxy, is shown in Fig. 3.

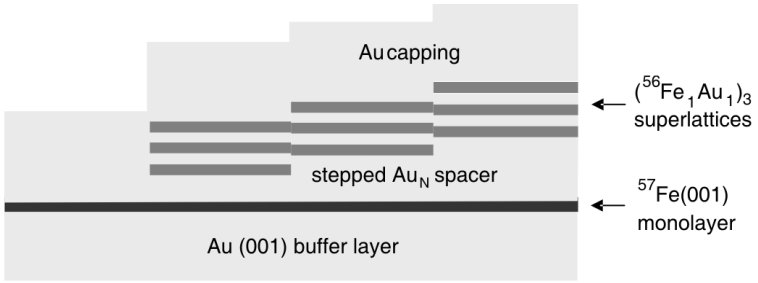

Fig. 3. Scheme of the $^{57}Fe_1/Au_N/(^{56}Fe_1Au_1)_3$ system grown on Au(001) and covered with Au

First, on the Au(001) buffer, a ^{57}Fe monolayer was deposited. Then, using a moveable shutter, a stepped spacer layer Au_N, with the thickness ranging from $N = 3$ to $N = 7$ monolayers (MLs) in one monolayer steps (1ML Au = 2.04 Å), was evaporated. The step width was 1 mm. On the spacer, a monoatomic $(^{56}Fe_1Au_1)_3$ superlattice was prepared by alternating evaporation of ^{56}Fe(001) and Au(001) atomic layers, while a part of the previously prepared system was kept shuttered to give access to the uncoupled Fe monolayer properties. Finally, the whole sample was capped with a 2 nm protective Au film. The sample was mounted in a He cryostat and oriented with the Au spacer step edges parallel to the direction of the X-ray propagation. Due to the fine horizontal focusing of the X-ray beam in the temperature dependent GI-NRS investigations, it was possible to collect the time spectra for different sample positions relative to the X-ray beam corresponding to the selected thickness of the Au spacer. In this way, the influence of the IEC on the Fe monolayer magnetic state was probed via the dependence of the monolayer hyperfine magnetic field on the spacer thickness. The time spectrum of the uncoupled Fe monolayer collected at 80 K is shown in Fig. 4 (curve a).

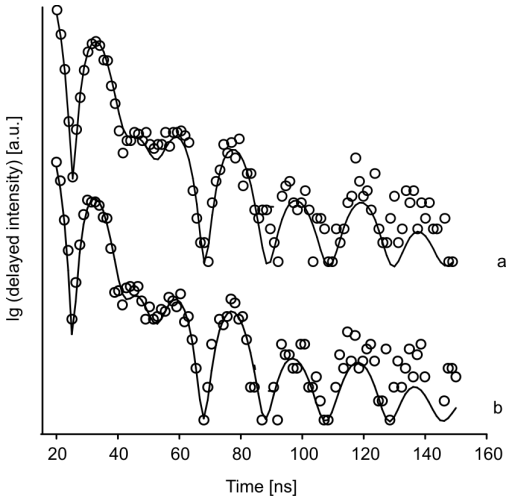

Fig. 4. Time spectra collected at 80 K for a) an uncoupled ^{57}Fe monolayer and b) for the $^{57}Fe_1/Au_4/(^{56}Fe_1Au_1)_3$ system. The solid lines represent theoretical fits

A satisfactory fit was obtained assuming three magnetic components characterized by the magnetic hyperfine field distributions (HFDs). The direction of all hyperfine magnetic fields, B_{HF}, was along the film normal, confirming the perpendicular magnetic anisotropy of the Fe monolayer. Interpretation of the beat pattern in terms of hyperfine parameters, as well as the relative contributions of the fitted components, agrees with the CEMS results of the Fe(001) monolayer grown on Au(001) [14]. At low temperatures, the time spectra measured for the coupled Fe monolayer were very similar and, within the statistical error, could be fitted with the same set of parameters, indicating negligible influence of IEC (see, for comparison, GI-NRS data of $^{57}Fe_1/Au_4/(^{56}Fe_1Au_1)_3$ shown in Fig. 4 (curve b)). This

situation changes as the Fe monolayer Curie temperature is approached, as seen from the time spectra measured at 200 K (Fig. 5). Similar to the 80 K data, the fits were obtained assuming three spectral components. All spectra were fitted simultaneously with the magnetic hyperfine field values and their HFDs as the only independent parameters.

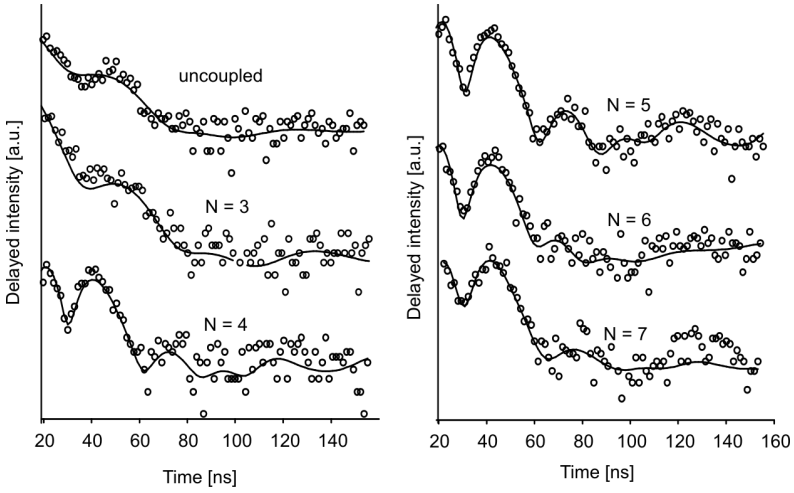

Fig. 5. Time spectra collected at 200 K for the uncoupled Fe monolayer and for $^{57}Fe_1/Au_N/(^{56}Fe_1Au_1)_3$ with different spacer thickness measured in the number N of Au(001) monolayers

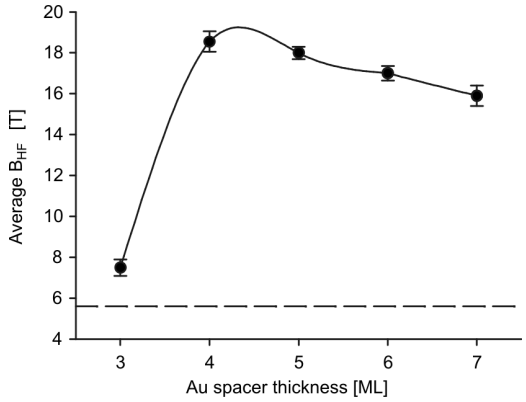

Fig. 6. Average hyperfine magnetic field $<B_{HF}>$ derived from the time spectra measured for the $^{57}Fe_1/Au_N/(^{56}Fe_1Au_1)_3$ system at 200 K in function of the Au spacer thickness. The dashed line indicates the uncoupled monolayer value. The solid line is a guide for the eyes only

Other parameters such as chemical shift, quadrupole splitting, and relative subspectra contributions (describing local structure), were treated consistently. In such a model, B_{HF} and its distribution are a measure of the local magnetization averaged over the scale given by the characteristic time window of the method (10^{-8} s) [8]. In

Figure 6, the average hyperfine magnetic field, $\langle B_{HF} \rangle$, obtained from the fit is shown in function of the spacer thickness. The dashed line marks the uncoupled Fe monolayer average hyperfine field ($\langle B_{HF} \rangle$ = 5.6 T). It is clear that the change of $\langle B_{HF} \rangle$ with the spacer thickness is non-monotonic, reflecting changes in the strength of the IEC which is ferromagnetic in the studied range of spacer thickness. Surprisingly, the closest proximity of the magnetic layer (N = 3) does not lead to the maximum hyperfine magnetic field enhancement. The maximum $\langle B_{HF} \rangle$ = 18.6 T was found for the 4 ML of Au spacer, and $\langle B_{HF} \rangle$ clearly decreases for the thicker spacers. The above results indicate that the magnetism of Fe(001) monolayers can be tuned by indirect exchange coupling to another magnetic system.

4. Fe(110) films on W(110)

For the epitaxial Fe(110) film on W(110), the archetypal system for studying ultrathin film magnetism, there are two different thickness regimes where the most intriguing properties have been found: i) ultrathin Fe films with thickness in the range of 0.5–4 ML, where the onset of ferromagnetic behaviour is expected [2], and ii) Fe films with thicknesses of a few tens of ML in the vicinity of the in plane spin reorientation transition (SRT) [15]. Using the UHV system at ID 18, the non-collinear magnetization structure in the ultrathin films region, as well as magnetization profiles during the in-plane SRT accompanying the film growth, these regimes could be studied with unprecedented spatial resolution.

As shown in Fig. 1b, ^{57}Fe could be deposited on a freshly cleaned and pre-aligned (to the X-ray beam) W(110) crystal. The first pseudomorphic monolayer was deposited at 600 K. The rest of the layer, beyond 1 ML, was deposited at room temperature, and all GI-NRS time measurements were also made at room temperature. Using a remote-operated shutter and a precision ^{57}Fe flux monitor, the whole preparation process could be operated on-line from the control hutch, without stopping the X-ray beam. Thus, the time of the experiment could be minimized, ensuring clean preparation and impurity-free films. It is also important that virgin magnetic states can be accessed, since, in contrast with most magnetic measurements, no magnetic field is necessary for the NRS. The measurement procedure that allows the acquisition of the GI-NRS time spectra along with the film deposition makes the method extremely fast. It was possible to complete the entire experimental run for the ^{57}Fe films in the thickness range 1.8 Å to 6.5 Å (step 0.4 Å) in 1.5 h.

Figure 7 shows a selection of the measured time spectra for $\mathbf{k}_0$ parallel to the $[1\,\bar{1}0]$ and [001] directions in the W(110) plane (left and right panels, respectively). The spectrum of the 1.8 Å film (corresponding to 1.1 pseudomorphic Fe(110) monolayer (psML)) shows no quantum beat pattern, in agreement with the literature data that the monolayer Curie temperature is of about 240 K [2]. A quantum beat structure that appears in the time spectra when the nominal Fe thickness reaches 3 Å, which corresponds to 1.8 psML, is of a magnetic origin. For this coverage, formation of the

magnetic double layer islands surrounded by the nonmagnetic monolayer areas is expected [16]. The similarity of the spectra measured for the two perpendicular in-plane W(110) directions indicates that the magnetization component perpendicular to the film plane dominates. Otherwise, due to uniaxial in-plane magnetic anisotropy expected for the Fe/W(110) by symmetry of the surface unit cell, the spectra should be very different (compare simulations in Fig. 2). The situation changes for coverage above 5Å (~3 psML), when, indeed, an in-plane magnetization component, with pronounced uniaxial anisotropy can be deduced from the clearly different spectra for the [001] and $[1\,\bar{1}\,0]$ directions. The above observation indicates that the thickness induced spin reorientation transition, from the out-of-plane to the in-plane magnetization direction, takes place, in agreement with the literature data. The numerical analysis of the measured time spectra should allow determination of the local magnetization profiles across the film which cannot be accessed by other methods.

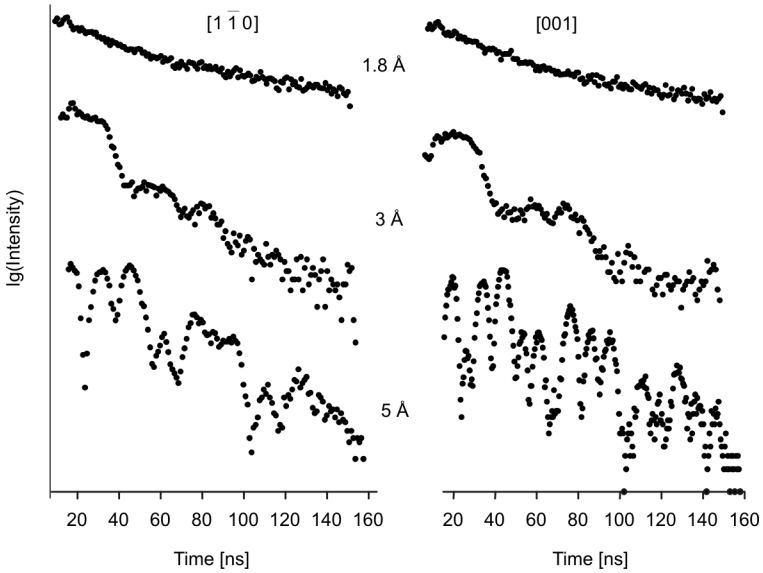

Fig. 7. Measured NRS time spectra of ultrathin ^{57}Fe films on W(110) for selected Fe coverage (in Å), for $\mathbf{k}_0$ parallel to $[1\,\bar{1}\,0]$ and [001] directions in the W(110) plane (left and right panels, respectively)

As mentioned above, because of the reduced surface symmetry, the Fe(110) films provide an example where in-plane surface anisotropies occur in addition to the usual out-of plane anisotropies. These in-plane anisotropies may induce an in plane SRT, as it was observed by Gradmann et al. in Fe(110) films on W(110), for film thicknesses between 30 and 50 ML, where the magnetization switching from [001] to $[1\,\bar{1}\,0]$ was found [15]. The nature of the transition is not fully explained. During the film growth, when approaching the critical film thickness, it can be considered either as continuous magnetization rotation from $[1\,\bar{1}\,0]$ to [001] or as coexistence of the $[1\,\bar{1}\,0]$ and [001]

oriented magnetic domains with different occupation. In-field measurements [17] or remanent measurements after saturating field pulses [18] point to the domain model. On the other hand, the early conversion electron Mössbauer study does not exclude the scenario of continuous rotation occurring without external field [15]. It is also plausible that the applied field could change the character of transition. The present GI-NRS experiment allowed us to get insight into the mechanism of the in plane SRT. In a single experimental run, multiple transition steps induced by the film thickness could be studied. Methodology of the thickness induced SRT studies was similar to that described above. ^{57}Fe was evaporated on the W(110) crystal held at 330 K with the rate of 0.3 ML/min to the final thickness of 30 ML. During the preparation, a set of NRS time spectra were collected (acquisition time per spectrum was only several seconds), thus probing the hyperfine parameters in 0.3 ML thickness steps.

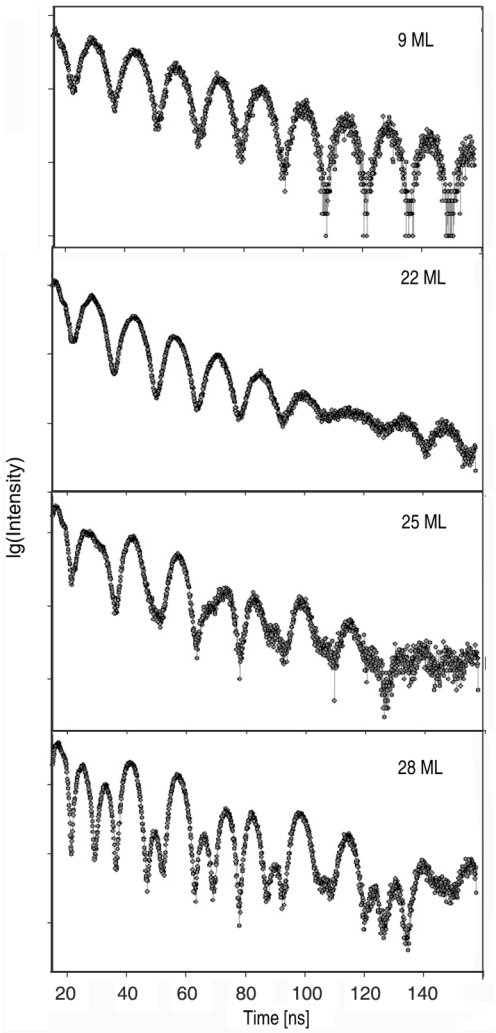

Fig. 8. NRS time spectra ($\mathbf{k}_0$ to $[1\,\bar{1}0]$) of selected ^{57}Fe/W(110) films, demonstrating in-plane SRT. The film thicknesses are given in monolayers (1 ML corresponds to 2 Å)

Figure 8 shows characteristic NRS time spectra for selected Fe thicknesses. A regular beat structure at about 10 ML represents domination of the film interior with $B_{hf} = 33$ T, uniformly magnetized along $[1\,\bar{1}0]$. Such a magnetization state persists up to above 20 ML. An additional spectral feature, a slow modulation of the delayed intensity, as exemplified in Fig. 8 for the 22 ML thickness, is the dynamical beat. The apparent beat period increases with increasing time after excitation and decreases with increasing effective thickness of the sample. Around 25 ML, the beat pattern changes essentially and corresponds to a unique $B_{hf} = 33$ T along [001]. Assuming a homogeneous magnetization depth profile across the Fe(110) films, the following models were considered for the magnetization transition from $[1\,\bar{1}0]$ to [001]: (i) coherent rotation and (ii) decay to [001] oriented domains. Both models show distinctly different spectra, as shown by simulations in Fig. 9, but, unfortunately, any combination of the magnetization configuration resulting from the models could give a satisfactory description of the NRS time spectra series in the thickness induced spin reorientation transition. This indicates a more complex nature of the transition, for example via non-collinear magnetization states.

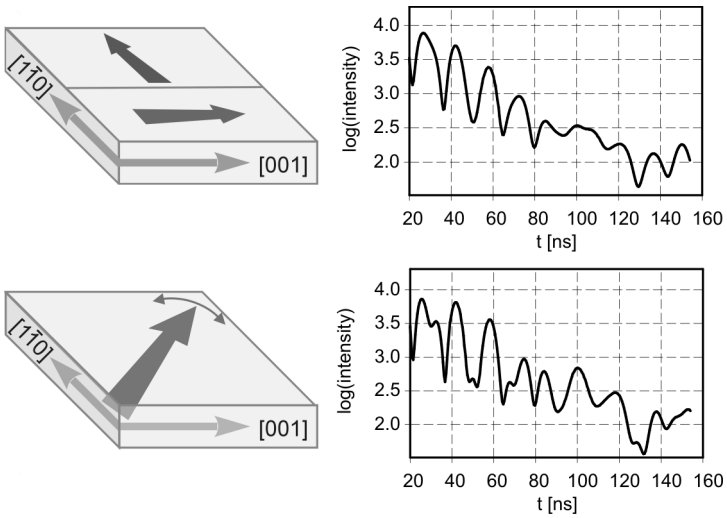

Fig. 9. Two models of in-plane SRT for an iron film on W(110) with a uniform magnetization along the film normal and corresponding simulated NRS time spectra

Summarizing, it was shown that GI-NRS is a powerful tool in studies of magnetism of low dimensional Fe-based systems. The method is now extremely sensitive and applicable under demanding UHV conditions, giving chance for *in-situ* dynamic studies of magnetization evolution in ultrathin films. NRS can be also applied to other classes of nanomaterials, such as clusters or biomolecules deposited on the surfaces. It should be possible to extend such applications to other isotopes with low-energy nuc-

lear transitions (below 30 keV), such as rare-earth isotopes ^{169}Tm, ^{151}Eu, ^{149}Sm, and ^{161}Dy, which are also of great interest for their magnetic properties.

Acknowledgements

This work was supported by the European Community under the Specific Targeted Research Project Contract No. NMP4-CT-2003-001516 (DYNASYNC), by the Austrian Federal Ministry of Education, Science and Culture under grant GZ 45.529/2-VI/B/7a/2002 (MDN project) and by the Polish Ministry of Education and Science. J.K. gratefully acknowledges professorial grant of the Foundation for Polish Science (FNP).

References

[1] PIETZSCH O., KUBETZKA A., BODE M., WIESENDANGER R., Phys. Rev. Lett., 84 (2000), 5212.
[2] ELMERS H.J., HAUSCHILD J., HOCHE H., GRADMANN U., BETHGE H., HEUER D., KOHLER U., Phys. Rev. Lett., 73 (1994), 898.
[3]LU L., BANSMANN J., MEIWES-BROER K.H.J., Phys. Cond. Matter, 10 (1998), 2873.
[4] ŚLĘZAK T., KARAŚ W., KROP K., KUBIK M., WILGOCKA-ŚLĘZAK D., SPIRIDIS N., KORECKI J., J. Magn. Magn. Matter., 240 (2002), 362.
[5] ELMERS H.J., HAUSCHILD J., GRADMANN U., Phys. Rev. B, 59 (1999), 3688.
[6] PRZYBYLSKI M., KORECKI J., GRADMANN U., Appl. Phys. A, 52 (1991), 33
[7] Hyperfine Interact., 123/124 (1999), Issue on Nuclear Resonant Scattering of Synchrotron Radiation, E. Gerdau, H. de Ward (Eds.); RÜFFER R., Hyperfine Interact. 141–142 (2002), 83.
[8] RÖHLSBERGER R., *Nuclear Condensed Matter Physics with Synchrotron Radiation,* STMP 208, Springer-Verlag, Berlin, 2004.
[9] STANKOV S., RÜFFER R., SLADECEK M., RENNHOFER M., SEPIOŁ B., VOGL G., SPIRIDIS N., ŚLĘZAK T., KORECKI J., Rev. Sci. Instr., 79 (2008), 045108.
[10] RÜFFER R., CHUMAKOV A.I., Hyperfine Interact. 97–98 (1996), 589; http://www.esrf.fr/exp_facilities/ID18/
[11] STURHAHN W., Hyperfine Interact. 125 (2000), 149.
[12] RÖHLSBERGER R., BANSMANN J., SENZ V., JONAS K.L., BETTAC A., MEIWES-BROER K.H., LEUPOLD O., Phys. Rev. B, 67 (2003), 245412.
[13] ŚLĘZAK T., ŚLĘZAK M., MATLAK K., ROHLSBERGER R., L'ABBE C., RÜFFER R., SPIRIDIS N., ZAJĄC M., KORECKI J., Surf. Sci., 601 (2007), 4300.
[14] KARAŚ W., HANDKE B., KROP K., KUBIK M., ŚLĘZAK T., SPIRIDIS N., WILGOCKA-ŚLĘZAK D., KORECKI J., Phys. Stat. Sol. A, 189 (2002), 287
[15] GRADMANN U., KORECKI J., WALLER C., Appl. Phys. A, 39 (1986) 101.
[16] WEBER N., WAGNER K., ELMERS H.J., HAUSCHILD J., GRADMANN U., Phys. Rev. B 55 (1997), 14121.
[17] ELMERS H.J., GRADMANN U., Appl. Phys. A, 51 (1990), 255.
[18] BAEK I.-G., LEE H.G., KIM H.-J., VESCOVO E., Phys. Rev. B, 67 (2003), 075401.

Received 16 May 2007